Exploration of a European-centered strawberry diversity panel provides markers and candidate genes for the control of fruit quality traits

Alexandre Prohaska, Pol Rey-Serra, Johann J. Petit, Aurélie Petit, Justine Perrotte, Christophe Rothan, Béatrice Denoyes

Horticulture Research

Horticulture Research, 2024, **11**: uhae137

https://doi.org/10.1093/hr/uhae137

Article

Exploration of a European-centered strawberry diversity panel provides markers and candidate genes for the control of fruit quality traits

Alexandre Prohaska[1,2], Pol Rey-Serra[1], Johann Petit[1], Aurélie Petit[2], Justine Perrotte[2], Christophe Rothan[1,*] and Béatrice Denoyes[1,*]

[1]Univ. Bordeaux, INRAE, UMR BFP, F-33140 Villenave d'Ornon, France
[2]Invenio, MIN de Brienne, 110 Quai de Paludate, 33000 Bordeaux, France
*Corresponding authors: E-mail: beatrice.denoyes@inrae.fr; christophe.rothan@inrae.fr

Abstract

Fruit quality traits are major breeding targets in cultivated strawberry (*Fragaria* × *ananassa*). Taking into account the requirements of both growers and consumers when selecting high-quality cultivars is a real challenge. Here, we used a diversity panel enriched with unique European accessions and the 50 K FanaSNP array to highlight the evolution of strawberry diversity over the past 160 years, investigate the molecular basis of 12 major fruit quality traits by genome-wide association studies (GWAS), and provide genetic markers for breeding. Results show that considerable improvements of key breeding targets including fruit weight, firmness, composition, and appearance occurred simultaneously in European and American cultivars. Despite the high genetic diversity of our panel, we observed a drop in nucleotide diversity in certain chromosomal regions, revealing the impact of selection. GWAS identified 71 associations with 11 quality traits and, while validating known associations (firmness, sugar), highlighted the predominance of new quantitative trait locus (QTL), demonstrating the value of using untapped genetic resources. Three of the six selective sweeps detected are related to glossiness or skin resistance, two little-studied traits important for fruit attractiveness and, potentially, postharvest shelf life. Moreover, major QTL for firmness, glossiness, skin resistance, and susceptibility to bruising are found within a low diversity region of chromosome 3D. Stringent search for candidate genes underlying QTL uncovered strong candidates for fruit color, firmness, sugar and acid composition, glossiness, and skin resistance. Overall, our study provides a potential avenue for extending shelf life without compromising flavor and color as well as the genetic markers needed to achieve this goal.

Introduction

Cultivated strawberry (*Fragaria* × *ananassa*), the most widely consumed small fruit worldwide, results from spontaneous hybridization in botanical gardens in France in the 18th century between two octoploid (2n = 8x = 56) species (*Fragaria chiloensis* and *Fragaria virginiana*) imported from the New World [1]. Since then, cultivated strawberry has been continuously improved through the introgression of alleles from wild progenitors creating an admixed population of interspecific hybrid lineages [2–4]. Recurrent hybridization contributed to maintain genetic diversity in the domesticated populations [4]. However, lower genetic diversity and heterozygosity can be observed in highly structured populations, which nevertheless show considerably improved yield, fruit weight, and firmness [5]. Current efforts, triggered by consumer demand for sweet and highly flavored strawberries [6, 7], are aimed at improving the sensory and nutritional quality traits of the fruit such as color [8] and flavor [9]. Another area for improvement is the extension of the storage period and the reduction of postharvest rot, both of which are linked to fruit firmness [7] and little-explored fruit surface properties [10]. Several fruit quality traits can be easily manipulated using advanced technology, such as genome editing, which has successfully been applied to create new alleles modifying various traits including fruit color, sweetness, and aroma [7, 11]. Other complex (e.g. fruit size) and/or little-studied (e.g. fruit glossiness) traits first require elucidation of their genetic architecture. Until recently, following initial studies [12, 13], the dissection of the genetic control of complex fruit quality traits in *F.* × *ananassa* has mainly been achieved by mapping quantitative trait locus (QTL) on genetic linkage maps of biparental [14–16] or multiparental [17] populations. Causal genetic variants have been identified for several QTL, leading to the design of genetic markers for marker-assisted selection (MAS) of strawberry varieties with, for example, improved fruit color [8, 18], and better aroma [9].

Complexity of the allo-octoploid genome of *F.* × *ananassa*, where up to eight homeo-allelic forms of the same gene can be found [19], has until recently hampered the mapping of QTLs on a given chromosome. Whole-genome sequencing of *F.* × *ananassa* [1] and, more recently, its progenitors [20], showed that the four subgenomes of *F.* × *ananassa* are derived from the diploids *Fragaria vesca* and *Fragaria iinumae* and from two extinct species related to *F. iinumae* [20, 21]. Genome sequence further enabled the design of a single-nucleotide polymorphism (SNP) 50 K array with selected chromosome-specific SNPs [22] allowing the high-resolution mapping of QTLs. A recent breakthrough has been the completion of haplotype-resolved genomes for five genotypes of *F.* × *ananassa*

Received: 4 March 2024; **Accepted:** 5 May 2024; **Published:** 14 May 2024; **Corrected and Typeset:** 1 July 2024

[9, 23–26]. These developments make it possible to exploit strawberry diversity through genome-wide association studies (GWAS), which scans the genome for significant associations between genetic markers and the trait studied [2]. It thus can help unveil beneficial alleles through the exploration and characterization of strawberry genetic resources, which display a wide genetic and phenotypic diversity [4, 27–29]. So far, GWAS has been done on collections mostly centered on North American strawberry populations [4, 29], which enabled the discovery of major QTLs controlling fruit weight, firmness, sweetness, and aroma [4, 9, 29–31]. It would certainly benefit from the exploration of other less well-characterized germplasm found in Europe [32], a historically active strawberry breeding center [6].

In this study, we explored by GWAS the genetic architecture of fruit quality in *F.* × *ananassa*. To this end, we used the unexploited genetic diversity found in traditional and modern European varieties, in comparison with the better described diversity of North American varieties and some Asian genotypes. Our results are consistent with recent insights into the evolution of modern strawberry varieties and detected major QTL recently described, e.g. for fruit firmness. Moreover, we detected new QTL for most of the 12 fruit quality traits studied and the underlying candidate genes (CG). An example of this are the QTL and strong CG for the little-explored glossy trait, which underpins the shiny appearance of all modern strawberry varieties and was found to co-localize with a skin resistance trait. Our results therefore highlight the richness of European collections as a source of genetic diversity for strawberry breeding.

Results

Population structure and genetic diversity of the diversity panel of cultivated strawberry

We analyzed a germplasm diversity panel comprising 223 accessions of cultivated strawberries (*F.* × *ananassa*) available at Invenio (South-West France) (Table S1). Unlike the main diversity panels studied to date, where the bulk of the panel was constituted by North American accessions [4, 28], our panel was mostly composed of European accessions from several countries, with French cultivars being by far the most represented (96 accessions). In addition, the panel comprised representative cultivars from North America including California and Florida, Japan, and other breeding programs around the world (Fig. 1A, Table S1). Many cultivars were released between the 1990s and nowadays, but the panel also accurately covered the whole modern breeding period (>1950s) and the early stages of strawberry breeding, with cultivars reaching as far as the beginning of the 19th century (Fig. S1). Thirty-two accessions from this panel were common with those from the study by Horvath et al. (2011) [32]. Accessions from the diversity panel were genotyped with the 50 K FanaSNP array [22]. A total of 38 120 SNPs were retained after filtering for minor allelic frequency (MAF) (<5%) and missing data (>3%).

To explore relationships among the 223 accessions, we first evaluated the population structure with STRUCTURE software. We identified three distinct genetic clusters (Fig. 1B, Table S1). Group 1 (G1) includes most of the older European cultivars and their more recent relatives, as well as some old American cultivars (Fig. 1B). This group is hereafter named the Heirloom & related group. Group 2 (G2) clusters essentially European, as well as 14 American cultivars mostly from North-East America (Maryland, New York, and Canada) and three out of five Japanese cultivars (Fig. 1B) and was therefore named the European mixed group. California and Florida cultivars, together with other European ones, have been identified in group 3 (G3) hereafter named the American & European mixed group. A large amount of admixture (<70%) was observed for each group, with 108 out of 223 accessions split across more than one group, with most of the admixture spread between G2 and G3 (Fig. 1B).

To further investigate population structure, we performed principal component analysis (PCA) of the 223 accessions using the 38 120 SNP markers (Fig. 1C). The first two dimensions (PC1, PC2) explained 8.2% and 4.7% of the structural variance, respectively. The three genetic groups were positioned at each vertex of the crescent shape. PC1 also reflected the temporal separation between G1 and the other two groups when cultivars were displayed according to year of release (Fig. 1D). The phylogenetic analysis (Fig. S2) was consistent with the structure (Fig. 1B) and PCA (Figs. 1C, 1D) analyses.

Genome-wide comparisons of nucleotide diversity (π) 'between genetic groups' revealed no clear loss of genetic diversity from G1 to G2 and G3 (Fig. 1E). At the chromosome level, the distribution of nucleotide diversity among groups was uneven, with several genomic regions associated with significant enrichment or loss. Of notice, some regions were associated with a sharp reduction in diversity in G2 and/or G3 compared with G1, e.g. the 23 233 kb to 29 635 kb region on chromosome 3D (Fig. 1F). Additional examples can be found on other chromosomes such as chromosomes 2C, 3B, and 6B (Fig. S3). Progression towards the most recent American and European cultivars also translated in local augmentation in linkage disequilibrium (LD), where LD (at $r^2 = 0.20$) increased from an average distance of 802 184 bp for G1 to 1 073 213 bp for G2 and 1 253 777 bp for G3 (Fig. 1G, Fig. S4).

We then combined the SNP data from our diversity panel with those from University of California Davis (UCD panel) [4] and United States Department of Agriculture (USDA panel) [27] to position our collection in relation with these studies. The PCA of the combined data revealed that the Invenio collection largely overlapped the two USA collections, with the exception of the extreme end of the PC1 corresponding to the UCD program and a small group of genotypes representing probable introgressions of wild accessions into the California panel (Fig. 1H, Fig. S5). The University of Florida (FL) program was less represented in the dataset and closer to the UCD program on the PCA. Japanese and Asian varieties were located at the center of the crescent. In addition, the PCA highlighted the enrichment of our panel in 171 unique accessions not found in the UCD and USDA panel, thus emphasizing its potential to find new phenotypic diversity for fruit quality traits in cultivated strawberry (Fig. 1H, Fig. S6). Heterozygosity decreased in California and Florida cultivars in comparison to European and Asian cultivars. Interestingly, heterozygosity was significantly higher in cultivars and advanced lines of Invenio and in recent European cultivars (released after 1980) (Fig. 1I).

Fruit quality traits in the diversity panel

A total of 12 fruit quality traits were investigated in the panel of 223 accessions (Table 1). Traits were related to fruit weight (FW); fruit appearance (COL, skin color; UCOL, uniformity of skin color; UFS, uniformity of fruit shape; ACH, position and depth of achenes); firmness (FIRM); composition (TA, titratable acidity; TSS, total soluble solids (Brix units), and BA, the deduced ratio (Brix/TA)); and skin properties (GLOS, glossiness; SR, skin resistance; BRU, bruisedness). Analyses were carried out over two consecutive years, with the exception of the FIRM and SR traits, which were assessed over a single year (Table 1).

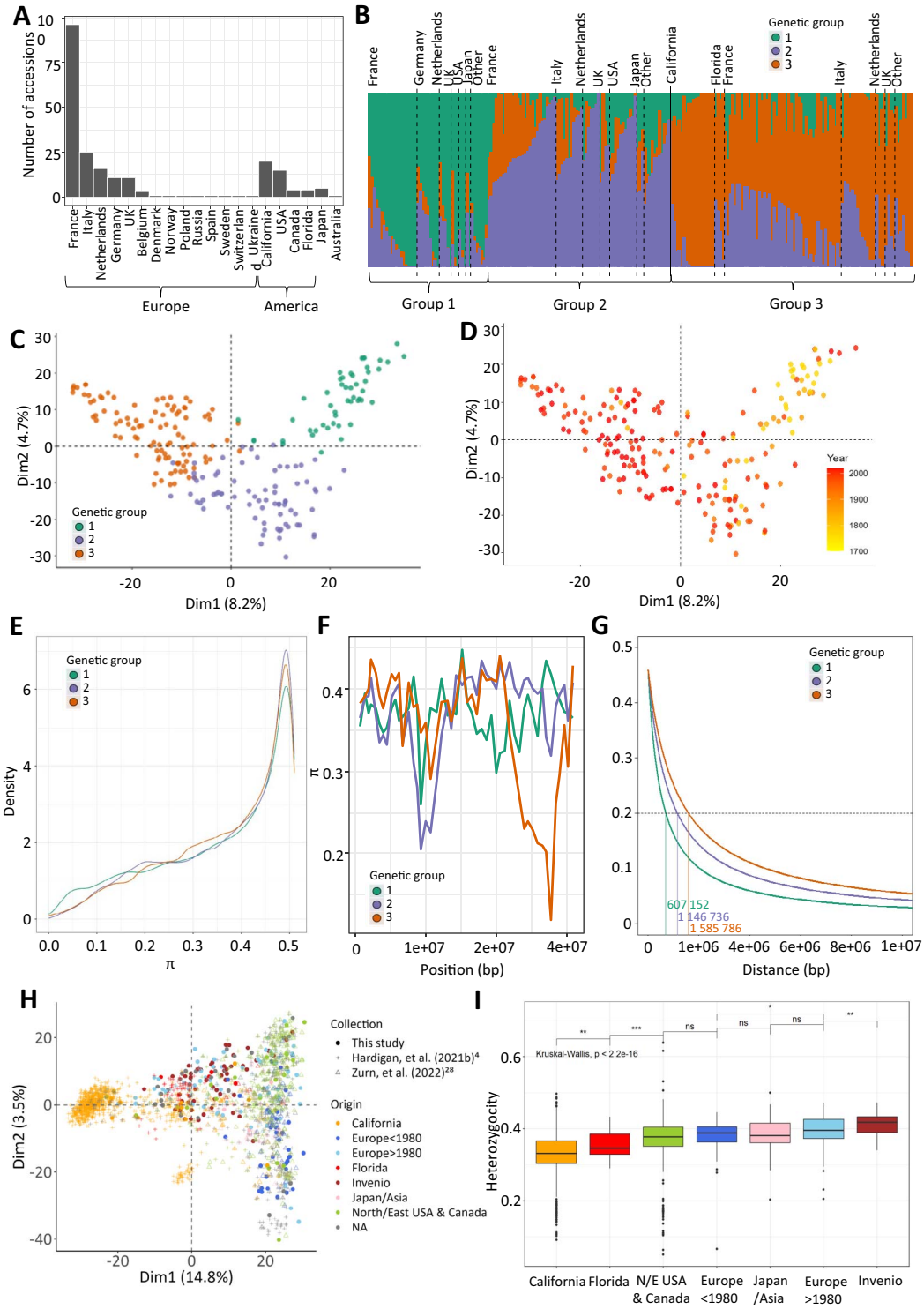

Figure 1. Genetic diversity of the panel. (A) Distribution of the geographical origin of the 223 accessions. (B) Structure barplot representing each genotype (bars) by its percentage of affiliation to each of the three genetic groups according to the STRUCTURE analysis. Individuals are sorted by genetic groups and geographical origins. (C,D) PCA of 38 120 SNP markers. Each accession (dot) is colored by its genetic group (C) or year of release (D). (E) Nucleotide diversity (π) distributions in windows of 400 kb across each genetic group. (F) π chromosome-wide estimates for each genetic group for 400 kb windows across the chromosome 3D. (G) LD decay along chromosome 1A. The dashed line represents the LD decay at $r^2 = 0.2$. (H) Distribution of the Invenio panel (filled dots) among 1569 genotypes (shaded dots) studied in Hardigan et al. (2021b) [4] and 539 genotypes studied in Zurn et al. (2022) [28] (shaded dots) with 3215 SNP markers. Accessions are colored according to geographical/breeding origin. (I) Heterozygosity coefficients across different geographical/breeding origins when combining accessions from the diversity panel and 1569 genotypes from Hardigan et al. (2021b) [4]. Genetic groups 1, 2, and 3 are colored in green, purple, and orange, respectively. Groups 1, 2, 3: Heirloom & related, European mixed group, and American & European mixed groups, respectively.

Table 1. Summary statistics of the 12 fruit quality traits evaluated on the diversity panel in 2020 and 2021.

Trait	Year	n	Range	Mean	σ	CV	H^2	H^2 G1	H^2 G2	H^2 G3	%GE	r^2 structure
Fruit weight (FW, g)	2020	169	1.8–30.9	12.4	5.4	43.6	0.96					
	2021	169	2.0–32.0	12.6	5.6	44.5	0.92					
	20–21	169	1.8–32.0	12.5	5.5	44.1	0.81	0.71	0.68	0.71	23.4	0.30
Shape uniformity (UFS)	2020	208	1–5	2.7	1.3	48.0						
	2021	197	1–5	3.1	1.3	41.5						
	20–21	208	1–5	2.9	1.3	44.9	0.26	ns	0.50	ns		0.05
Achene position (ACH)	2020	209	1–5	3.5	0.8	23.3						
	2021	198	1–5	3.2	0.9	28.8						
	20–21	209	1–5	3.4	0.9	26.2	0.66	0.71	0.67	0.60		0.08
Skin color (COL)	2020	201	1–7	1.2	4.507	3.7						
	2021	209	1–7.5	1.2	4.535	3.8						
	20–21	209	1–7.5	1.2	4.522	3.8	0.68	0.77	0.67	0.60		0.03
Color uniformity (UCOL)	2020	208	1–5	3.0	1.3	42.7						
	2021	198	1–5	2.8	1.3	47.0						
	20–21	208	1–5	2.9	1.3	44.9	0.43	ns	0.59	0.32		0.10
Firmness (FIRM, in kg/mm)	2020											
	2021	210	1.04–0.07	0.433	0.2	40.3	0.98	0.94	0.97	0.95		0.44
	20–21											
Titratable acidity (TA, in g / L)	2020	195	0.7–2.3	1.4	0.3	20.6	0.83					
	2021	175	0.4–2.0	1.2	0.3	24.1	0.91					
	20–21	195	0.4–2.3	1.3	0.3	23.1	0.70	ns	0.85	0.82	34.5	0.03
Total soluble solids (TSS, in Brix)	2020	207	3.6–11.0	7.1	1.4	19.7	0.92					
	2021	184	3.2–11.8	6.9	1.5	22.1	0.94					
	20–21	207	3.2–11.8	7.0	1.5	20.9	0.78	0.68	0.83	0.75	30.2	0.04
Brix/acidity ratio (BA)	2020	195	2.9–7.9	5.1	1.0	19.9	0.87					
	2021	175	2.1–12	5.6	1.5	27.5	0.95					
	20–21	195	2.1–12	5.3	1.3	24.8	0.54	ns	0.85	0.51	48.5	0.00
Glossiness (GLOS)	2020	195	1–5	3.5	1.2	35.8						
	2021	182	1–5	3.5	1.1	31.8						
	20–21	195	1–5	3.5	1.2	33.8	0.77	0.76	0.64	0.43		0.48
Skin resistance (SR)	2020											
	2021	210	0–3	1.65	1.0	58.2						0.34
	20–21											
Bruisedness (BRU)	2020	199	1–5	2.5	1.3	50.8						
	2021	54	0–5	1.8	1.0	54.3						
	20–21	199	0–5	1.9	1.1	55.7	0.57	0.52	0.45	ns		0.49

n, number of accessions; CV, Coefficient of Variation; H^2, broad sense heritability; %GE, percentage of genotype-by-environment interactions in the total variance; r^2 structure, structuration of the trait as the coefficient of determination of the linear regression between the trait values and the genetic groups; ns, not significant genotypic effect.
20–21 indicates the combined values across two years, 2020 and 2021.

Most of the traits exhibited a considerable range of variation in the diversity panel, with coefficients of variation ranging from 3.7% for COL to 58.2% for skin resistance. For example, FW (average: 12.5 g) ranged from 1.8 to 32 g. (Table 1). Most traits showed a normal distribution, while SR, GLOS, UFS, and BRU showed a skewed distribution (Fig. S6). Nine traits displayed high amount of genotypic variance associated with high broad sense heritability (H^2) ranging from 0.66 (ACH) to 0.98 (FIRM); H^2 of four traits, namely UFS (0.26), UCOL (0.43), BA (0.54), and BRU (0.57), was <0.6 (Table 1). Few variations of H^2 between groups were observed for FW and FIRM, suggesting that phenotypic variability was equivalent between groups, whereas a strongest decrease in H^2 was observed for GLOS and BRU in G3 (Table 1). A significant interaction between genotype and environment was detected for all the traits for which repeated measurements were available over 2 years (Table 1), with the effect of environment being strongest for traits related to fruit composition (TSS, TA, BA).

To further explore the phenotypes of the diversity panel, we performed a PCA of the 223 accessions using a PCA biplot (Fig. 2A). PC scores revealed that the three genetic groups were distributed differently according to PC1 (39.2%) and PC2 (17.2%) in terms of fruit quality traits. G1 was distinct from G2 and G3 (Fig. 1B, Fig. S7A). Examination of the loadings of the traits on PC1 further showed that FW, appearance (UFS, UCOL), FIRM, and skin properties (GLOS, SR, and BRU) traits were responsible for the separation between G1 on one side and G2 and G3 on the other side. TSS, TA, and ACH had a very small contribution to the differentiation of the three subpopulations along PC1, and mostly contributed to PC2 and PC3, respectively (Fig. 2A, Fig. S7B).

Correlation analysis of fruit quality trait data collected over 2020 and 2021 (Fig. 2B, Table S2) supported the relationships identified in the PCA biplot (Fig. 2A). GLOS, SR, and BRU traits were positively and strongly correlated with each other and with FW and FIRM ($r = 0.51$–0.87), indicating the strong potential for directional selection of these traits (Fig. 2A). UFS and UCOL were also highly correlated among them ($r = 0.64$) and, to a lesser extent ($r = 0.35$ and 0.26), with FW. TSS and TA were significantly correlated ($r = 0.45$) but, within groups, the correlation was only significant for G2 ($r = 0.51$) and G3 ($r = 0.47$) groups (Fig. S8). FW also demonstrated significant negative correlations with TSS ($r = -0.21$) and TA ($r = -0.15$) (Fig. 2B; Table S2). No or weak correlations were observed between ACH and other fruit quality traits.

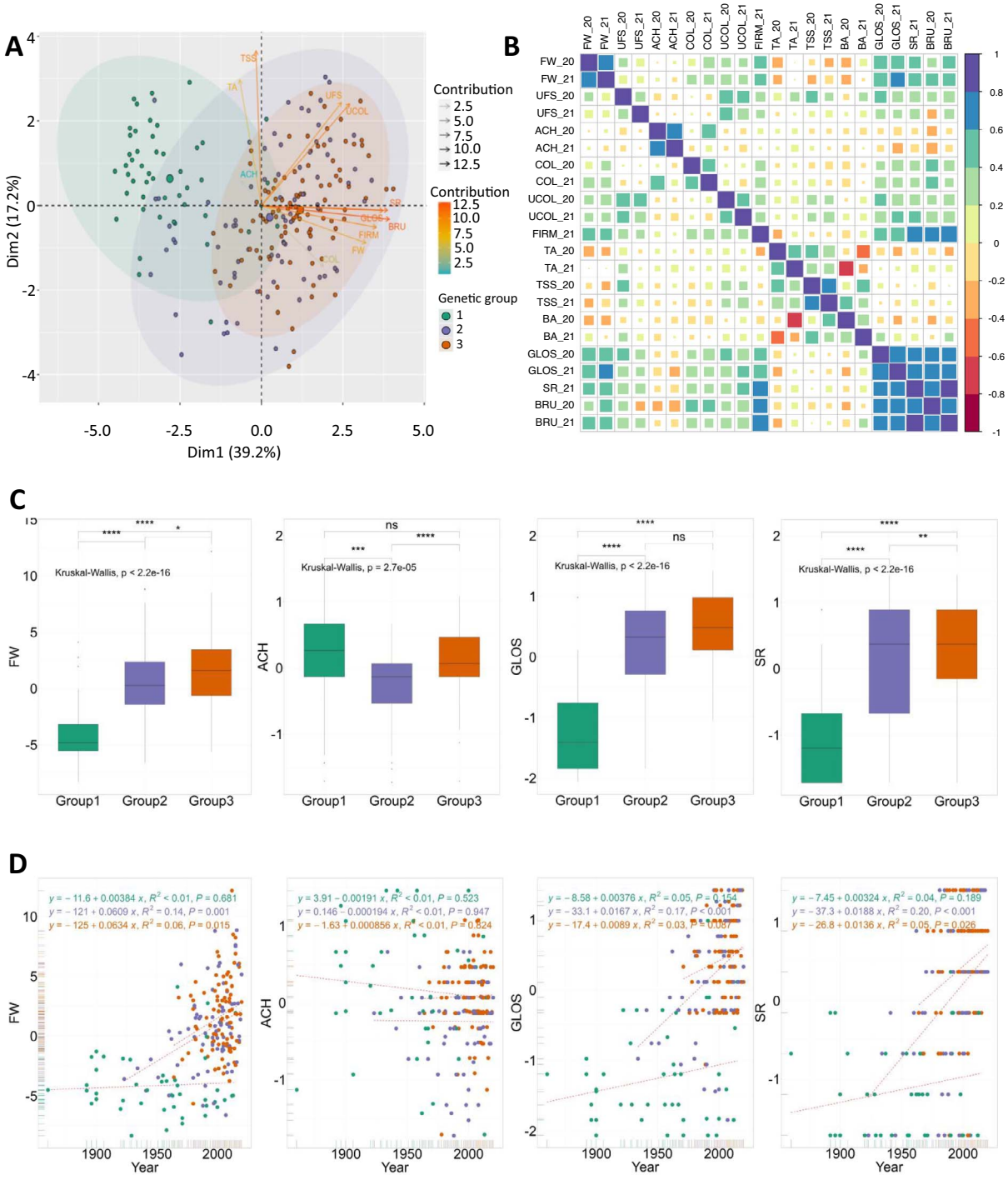

Figure 2. Phenotypic variations across the three genetic groups of the panel. (A) PCA of the 2-year BLUP values for 11 traits. (B) Correlations between the 12 traits for each year. (C) Comparisons of 2-year BLUP values for FW, ACH, GLOS, and SR among genetic groups. (D) Genetic gains for FW, ACH, GLOS, and SR among genetic groups. Genetic groups 1, 2, and 3 are colored in green, purple, and orange, respectively. Groups 1, 2, 3: Heirloom & related, European mixed group, and American & European mixed groups, respectively.

Most fruit quality traits have undergone significant phenotypic changes over time, as old varieties have evolved into modern cultivars (Figs. 2C, 2D, Fig. S9). Phenotypic values of all fruit quality traits, except BA and COL, were significantly different between the three genetic groups. For example, FW considerably increased during the modern breeding phase, as reflected mainly in trends within G2 and G3 (Figs. 2C, 2D). G1 was associated with low FW, dull, soft, low SR and easily wounded skin with uneven color and shape, whereas G3 exhibited the highest values for these traits (Fig. 2C, Fig. S9). G2 was equivalent to G3 for UFS and UCOL, TSS and TA, and GLOS; and was in the average of G1 and G3 for FW, FIRM, SR, and BRU. Cultivars from G2 displayed more outcropped achenes than the others (Fig. 2C, Fig. S9).

These changes are linked to significant genetic gains over time for most fruit quality traits, with the exception of ACH and BA (Fig. 2D, Fig. S10). For G2 and G3, the traits most affected along the breeding cycles were fruit appearance (GLOS, Fig. 2D; UFS

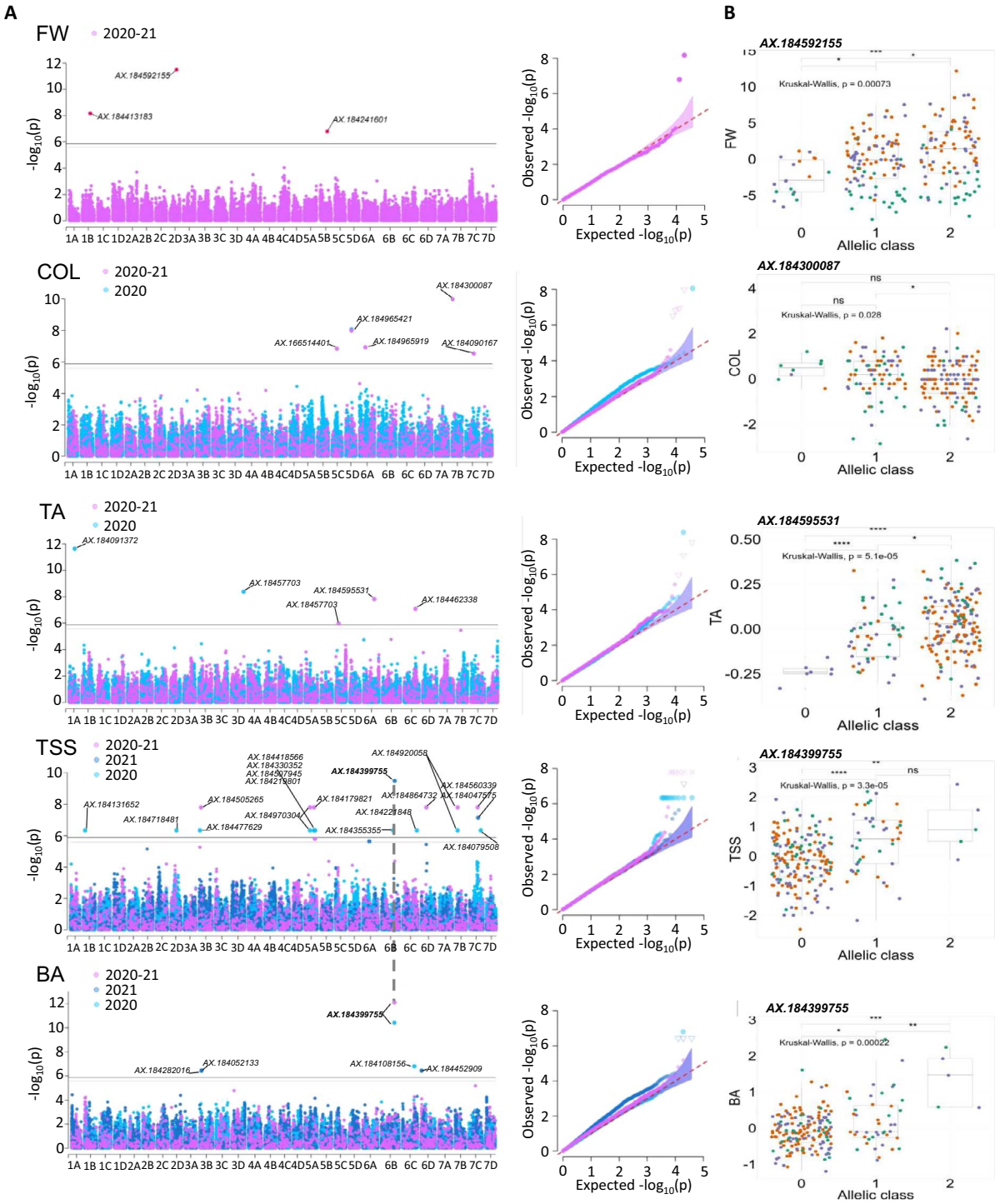

Figure 3. Genome-wide association study of FW, COL, TA, TSS, and BA. (A) Manhattan and Q-Q plots for yearly and 2-year BLUP values. (B) Effect of the most significant SNP marker. Genetic groups 1, 2, and 3 are colored in green, purple, and orange, respectively. Groups 1, 2, 3: Heirloom & related, European mixed group, and American & European mixed groups, respectively. Marker classes are as follows: 0 = AA genotype, 1 = AB, and 2 = BB genotype according to the Axiom™ Strawberry FanaSNP 50 k.

and UCOL, Fig. S10), fruit resilience to transport and postharvest storage (SR, Fig. 2D; BRU and FIRM, Fig. S10) and fruit weight (FW, Fig. 2D). These traits are important for consumers, retailers, and growers, respectively. A negative, non-significant trend was however observed for TSS and TA, whose values were lower in G2 and G3 than in G1 (Fig. S9). Remarkably, regardless of the TSS and TA reduction in modern varieties compared to old varieties, no significant differences for BA values were observed between groups (Fig. S9).

While positive and time-dependent genetic gains were observed within G2 and G3, genetic gains were usually low or inexistent within G1. For FW, for example, several recent varieties of the G1 showed the same trait values as old ones. The absence of major improvements for such traits in modern cultivars

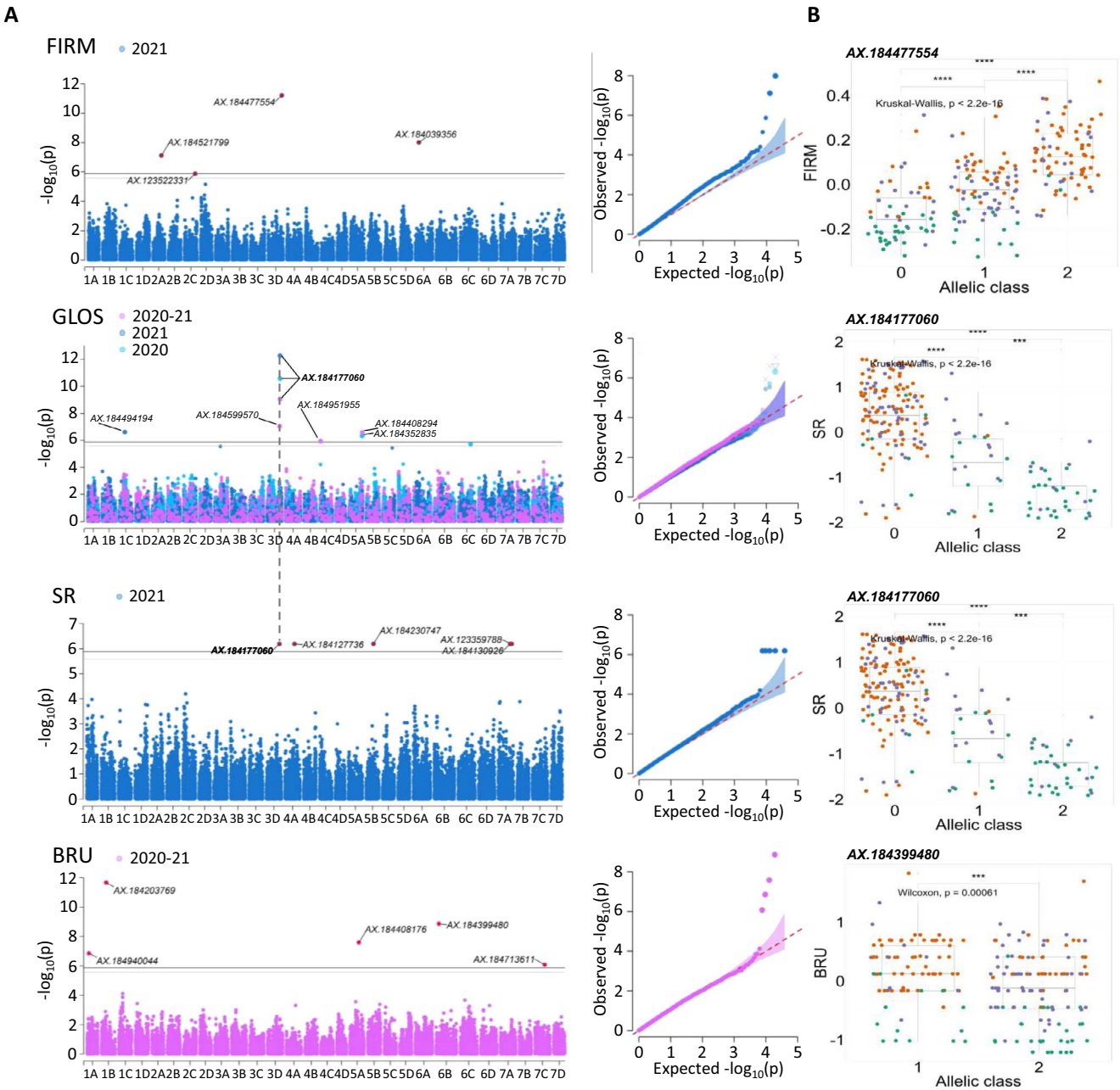

Figure 4. Genome-wide association study of FIRM, GLOS, SR, and BRU. (A) Manhattan and Q-Q plots for yearly and 2-year BLUP values. (B) Effect of the most significant SNP marker. Genetic groups 1, 2, and 3 are colored in green, purple, and orange, respectively. Groups 1, 2, 3: Heirloom & related, European mixed group, and American & European mixed groups, respectively. Marker classes are as follows: 0 = AA genotype, 1 = AB, and 2 = BB genotype according to the Axiom™ Strawberry FanaSNP 50 k.

belonging to G1 is probably due to a low selection pressure, as the main selection objective was to produce ornamental plants with pink flowers ('Frel' and 'Toscana') or white fruits ('Anablanca', 'Blanche_du_Morvan', 'F_Eure_et_Loire').

GWAS of fruit quality traits

To reveal the genetic architecture of fruit quality in strawberry, we performed GWAS on the 12 fruit quality traits assessed in the 223 accessions of the strawberry diversity panel using genome-wide SNP markers from the 50 K FanaSNP array [22]. The structuration of the population (Figs. 2B, 2C) was considered by fitting both kinship and structure as cofactors for GWAS analysis. Detailed Manhattan plots for all 12 traits are shown in Figs. 3, 4, Fig. S11. The 71 significant associations with SNP markers are distributed on 51 chromosomal regions spread on 23 chromosomes (Table S3).

Fruit weight and appearance (FW, UFS, COL, UCOL, ACH)

Three significant SNP were identified for FW on chromosome 1B (19 119 571 bp, *P*-value 6.74E-09), 5B (17 045 086 bp, *P*-value 1.60E-06) and a highly significant SNP on chromosome 2D (15 565 564 bp, *P*-value 3.27E-12) (Fig. 3A, Table S3). The minor allele of AX-184592155 had a phenotypic variance explained (PVE) of 11.8% with an effect of 1.8 g on FW (Fig. 3B, Table S3). Sixteen unique significant SNPs were identified for appearance traits, eight for UFS, three for ACH, and five for COL (Fig. 3A, Fig. S11, Table S3). No signal was detected for UCOL.

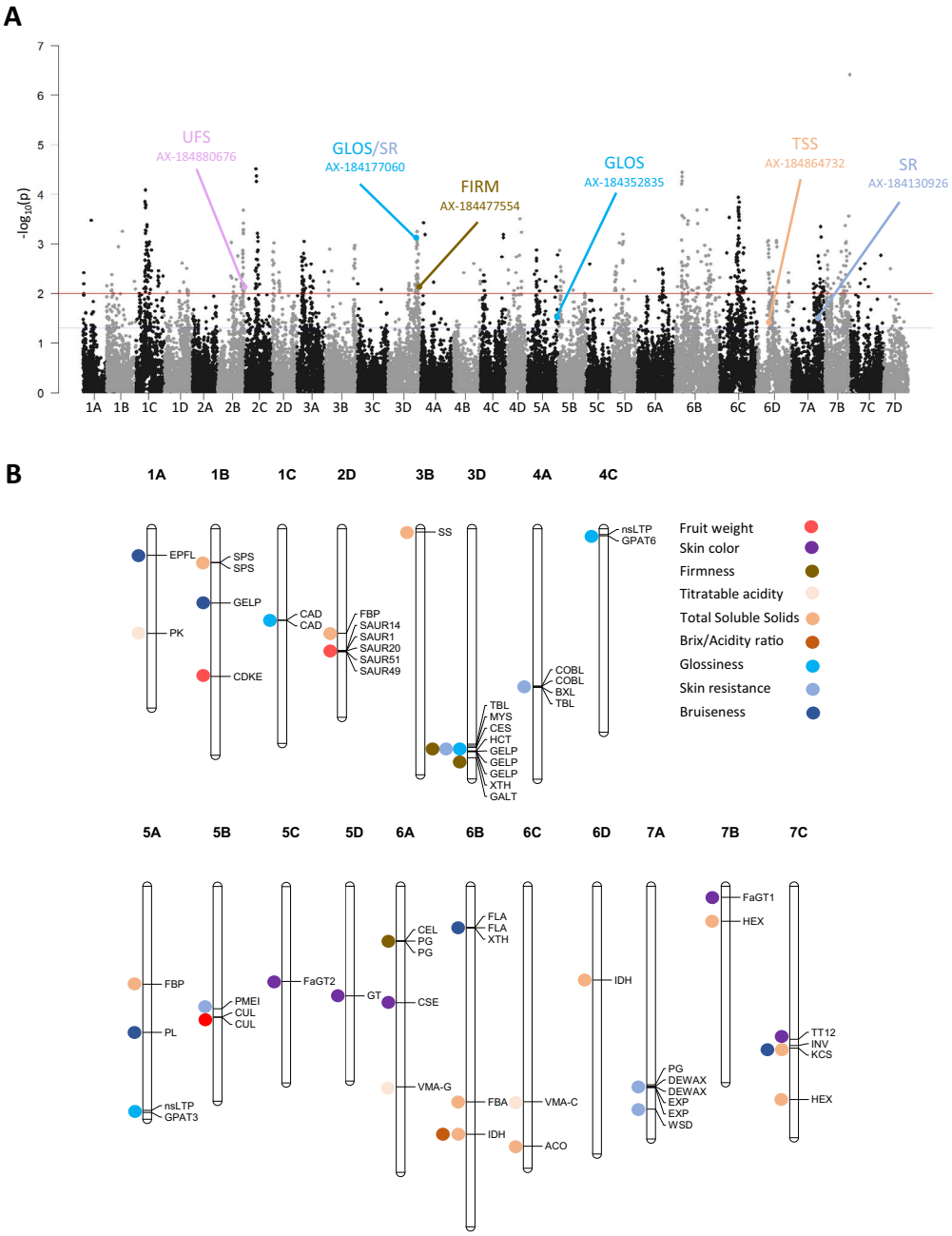

Figure 5. Selective sweeps and candidate genes. (A) Selective sweeps as a Manhattan plot of *P*-values of the genome scan based on Mahalanobis distance. Red and blue lines indicate thresholds at 0.01 and 0.05, respectively; trait associations with a *P*-value <.05 are indicated with colors. Only significant ($P < .05$) SNP markers associated with fruit quality QTL are represented. (B) Physical mapping of the candidate genes underlying the GWAS of nine traits on the Camarosa genome. Full names and abbreviations of candidate genes are given in Table 2.

Fruit composition (TA, TSS, BA)

Twenty-seven unique significant SNPs were detected for fruit composition traits, five for TA, 18 for TSS, and five for BA (Fig. 3A, Table S3). The SNP AX-184595531 detected for TA on the 2020–21 combined values (25 621 066 bp, *P*-value 1.55E-08) was particularly notable for its PVE of 35.5%. Only seven cultivars, all belonging to G2, were unfavorable homozygous for this marker (Fig. 3B). SNPs AX-184091372 on chromosome 1A (13 540 517 bp, *P*-value 2.30E-12, PVE 17.1%) and AX-184457703 on chromosome 3D (25 621 066 bp, *P*-value 4.22E-09, PVE 17.9%) were also of particular interest for their PVE and impacting effect on TA in 2021. AX-184399755 was the highest effect SNP for TSS in 2021 on chromosome 6B (31 578 303 bp, *P*-value 3.24E-10, PVE 19%) (Fig. 3B). It was also highly significant for BA in 2020 (*P*-value 3.84E-11, PVE 46.1%) and 2020–21 combined values (*P*-value 7.88E-13, PVE 65.8%) (Fig. 3B). Only five cultivars were favorable homozygous for this marker. Interestingly, the SNP markers associated with the TSS QTL on 6B (AX-184399755) and 6D (AX-184864732), and 7B (AX-184920058) and 7C (AX-184079508), were found very close on the diploid *F. vesca* reference genome (*F. vesca* v4.0.a1 [33]), at 606797 bp (Fvb6) and 449 220 bp (Fvb7) from each other, respectively.

Fruit firmness and skin properties (FIRM, GLOS, SR, BRU)

Four significant SNPs were detected for FIRM, six for GLOS, five for SR, and five for BRU (Fig. 4A, Table S3). The chromosome 3D was of particular interest for these traits as it comprises one highly

significant SNP for FIRM (29 275 014 bp, *P*-value 6.07E-12, PVE 11.2%) and the highly significant SNP AX-184177060 (27 845 440 bp) common to both GLOS (*P*-value 9.01E-10, PVE 26.2% on combined values) and SR (*P*-value 6.45E-07, PVE 8.4%) (Fig. 4B). The latter SNP was detected systematically in 2020, 2021, and 2020–21 for GLOS with PVE ranging from 26.2% to 28.7%, with a negative effect of the minor allele (−0.7 to −0.8 on 1–5 scale). MAF of this SNP was highly reduced toward G3, indicating strong selection of the favorable allele (Fig. 4B). SNPs for BRU were detected for the 2020–21 combined values only.

Selective sweep signals during strawberry improvement

We identified markers under selection during strawberry improvement in light of genome scans based on Mahalanobis distance across the diversity panel (Fig. 5A) and nucleotide diversity throughout the genome for all of the accessions in the diversity panel (Fig. 1F, Fig. S3). Seven significant associations of SNP markers with fruit quality QTL were detected, including one for UFS, one for FIRM, one for TSS, two for GLOS, and two for SR (Fig. 5A, Table S4). The AX-184177060 marker associated with GLOS and SR (chromosome 3D), the AX-184477554 associated with FIRM (chromosome 3D), and the AX-184864732 (chromosome 6D) associated with TSS, are found in chromosomal regions displaying a drastic reduction in nucleotide diversity in modern genotypes (Fig. 1F, Fig. S3, Table S4). For example, in the case of the SNP marker AX-184177060 associated with the SR and GLOS QTL, the favorable allele is over-represented in the most recent accessions (average year of release 2000), whereas cultivars heterozygous or unfavorably homozygous for the marker were released ∼1967 and 1947, respectively. This finding supports the fact that the favorable allele has been selected over time.

Candidate genes were identified for 37 QTL controlling 9 fruit quality traits

CG underlying fruit quality QTL were identified within a window of ∼400 kb surrounding the QTL marker. This value, which corresponds to the short-range LD found in the California cultivars of *F.* × *ananassa* [4], is stringent compared to the average LD calculated on the 28 linkage groups in our diversity panel, which is 932 kb. In chromosomal regions harboring strong QTL of interest and displaying low genetic diversity and high LD, i.e. the 3D region extending from 23 233 to 29 635 kb (Fig. 1F), we considered much larger intervals based on LD estimates (up to ∼1382 kb) for 3B and 3D. We excluded two traits (UFS and ACH) from CG analysis because the molecular pathways underlying these traits are far from being deciphered in strawberry. No QTL was detected for UCOL. In total, we identified 64 candidate loci for 37 SNP markers associated with the nine fruit quality traits (Fig. 5B). Table 2 provides names, abbreviations, and positions on Camarosa and Royal Royce genomes of these 64 CG. Their possible functions are indicated in Table S5.

Discussion

Genetic and phenotypic shifts in modern strawberry breeding programs

Our study sheds light on the genetic and phenotypic shifts that occurred over the last 160 years of strawberry breeding by analyzing 223 accessions comprising original old and modern European breeding material. According to our analyses, old strawberry cultivars, which here consist mainly of European cultivars selected before 1950 and included in the Heirloom & related group (G1), are clearly separated from other genetic resources (Fig. 1C), in agreement with earlier studies [32] confirmed in recent papers [4, 34]. For over half a century [35], breeding programs in Western and Southern Europe have made extensive use of California cultivars and, more recently, of Florida cultivars, which are underrepresented in our study, as progenitors. As a consequence, our results show the clustering of most European recent cultivars in an American & European mixed group (G3). The European mixed group (G2), which includes other European cultivars, is likely related to the group previously named Cosmopolitan [4]. European cultivars were also separated from US cultivars in the Zurn et al. (2022) study [28] due to the large number of American accessions.

The overall nucleotide diversity is well conserved among the genetic groups of our panel (Fig. 1E). In contrast, a significant erosion of genetic diversity was observed in highly structured populations [4, 5, 29]. We found a more nuanced picture by examining nucleotide diversity at the chromosome level, since it drops dramatically in regions potentially subject to selection pressure (Fig. 1F, Fig. S3). The decrease in both LD and heterozygosity specifically observed in the most recent American cultivars [4] is likely explained by the gradual differentiation of California and Florida populations. In contrast, cultivars and advanced lines of Invenio as well as the recent European cultivars released after 1980 display higher heterozygosity values (Fig. 1I). One possible explanation for the high genetic diversity retained in European accessions is that European breeders had to cope with a wide range of breeding targets due to the diversity of cultural practices, markets, and consumer preferences found in Europe [6, 36]. High-quality strawberry varieties released in Europe therefore had to meet the requirements of both high cultivar performance, e.g. high fruit yield, as in California cultivars [5] and high sensory fruit quality, e.g. high flavor [6].

Remarkably, recent studies have shown that despite a loss in genetic diversity, increases in both genetic gain and phenotypic variation were observed in highly structured populations such as those of the California breeding programs [5]. In these programs, breeding efforts rapidly led to the improvement of fruit weight and fruit firmness [5, 27, 29], which participated in the so-called California green revolution [5]. European breeding programs have benefited from these efforts, as modern American cultivars appear in the pedigree of prominent European cultivars [3]. Consistently, our results indicate a similar trend towards improved fruit size and firmness, as well as skin glossiness and resistance, in recent European germplasm (Fig. 2C, Fig. S9). Interestingly, we found that TSS and TA values decreased over time in G1 but that the BA ratio kept the same value (Figs. S9, S10), in agreement with Feldmann et al. (2024) [5], who even observed an increase in BA levels, which could partly counterbalance the decrease in fruit sweetness. Antagonism between yield and firmness, on one side, and TSS and TA, on the other side, was previously reported [5, 27, 31].

Novel markers for the selection of fruit quality traits

GWAS is a powerful tool for the detection of SNP markers linked to different traits in strawberry [9, 17, 29, 31, 37, 38]. Here, based on a large diversity panel, we detected 71 marker associations to major fruit quality breeding targets. Some of the marker/QTL associations detected confirm published results and, consequently, validate our findings in a different genetic context. In comparison with the GWAS/QTL published data [4, 15, 17, 29, 31, 39–41] obtained using the Affymetrix strawberry arrays, only two common fruit quality QTL located on the same chromosomal

Table 2. Candidate genes underlying nine fruit quality traits.

Trait	Chr	PVE	SNP marker	Position Camarosa	Position Royal Royce	Protein encoded by the Candidate Gene (CG)	CG abbreviation	CG position Camarosa	F. × ananassa identity	TAIR Arabidopsis homolog	Published strawberry GWAS/QTL a
Fruit weight (FW)	1B	5.5	AX-184413183	19 119 571	15 971 709	Cyclin-dependent kinase E-1	*CDKE*	18 842 135	FxaC_2g34880	AT5G63610.1	
	2D	11.8	AX-184592155	15 565 564	8 801 569	Small auxin upregulated RNA 14	*SAUR14*	15 581 781	FxaC_8g28530	AT4G38840.1	
						Small auxin upregulated RNA 1	*SAUR1*	15 594 644	FxaC_8g28550	AT4G34770.1	
						Small auxin upregulated RNA 20	*SAUR20*	15 611 587	FxaC_8g28590	AT5G18020.1	
						Small auxin upregulated RNA 51	*SAUR51*	15 687 585	FxaC_8g28690	AT1G75580.1	
						Small auxin upregulated RNA 49	*SAUR49*	15 697 093	FxaC_8g28700	AT4G34750.2	
	5B	3.6	AX-184241601	17 045 086	10 918 733	Cullin	*CUL*	16 733 799	FxaC_18g25221	AT4G02570.4	
						Cullin	*CUL*	16 708 079	FxaC_18g25150	AT4G02570.4	
Skin color (COL)	5C	1.7	AX-166514401	11 987 143		Anthocyanidin 3-O-glucosyltransferase	*FaGT2*	12 158 604	FxaC_19g22400	AT5G17050.1	
	5D	3.8–23.4	AX-184965421	14 022 053	13 542 145	Flavonoid 3-O-glycosyltransferase	*GT*	14 049 628	FxaC_20g25430	AT5G54010.1	
	6A	2.6	AX-184965919	14 476 176	21 070 121	Caffeoylshikimate esterase	*CSE*	14 923 586	FxaC_21g30560	AT1G52760.1	
	7B	3.01	AX-184300087	1 386 945	23 020 879	Anthocyanidin 3-O-glucosyltransferase	*FaGT1*	1 422 660	FxaC_26g03070	AT5G17050.1	
	7C	9.9	AX-184090167	19 438 028	13 528 856	TT12-like MATE transporter	*TT12*	19 581 584	FxaC_27g28060	AT4G00350.1	
Firmness (FIRM)	3D	11.2	AX-184477554	29 275 014	2 454 715	AGP galactosyltransferase	*GALT*	29 300 471	FxaC_12g45150	AT4G21060.2	
						∗ Xyloglucan endotransglucosylase/hydrolase	*XTH*	28 520 127	FxaC_12g43560	AT3G23730.1	
						∗ Cellulose synhase	*CES*	27 994 587	FxaC_12g42810	AT4G18780.1	
	6A	6.3	AX-184039356	7 277 130	27 533 782	Cellulase 1	*CEL*	7 038 578	FxaC_21g15730	AT1G70710.1	Cockerton et al. (2021); Hardigan et al. (2021b); Fan et al. (2024); Muñoz et al. (2024)
						Polygalacturonase	*PG*	7 048 245	FxaC_21g15750	AT3G07820.1	
						Polygalacturonase	*PG*	7 054 511	FxaC_21g15770	AT3G07820.1	
Titratable acidity (TA)	1A	17.1	AX-184091372	13 540 517	13 469 152	Pyruvate kinase	*PK*	13 355 376	FxaC_1g27460	AT2G36580.1	
	6A	35.3	AX-184595531	25 621 066	9 172 070	V-type proton ATPase subunit G	*VMA-G*	25 704 934	FxaC_21g49700	AT3G01390.4	
	6C	6.8	AX-184462338	27 458 040		V-type proton ATPase subunit C	*VMA-C*	27 580 375	FxaC_23g44340	AT1G12840.1	

(Continued)

Table 2. Continued

Trait	Chr	PVE	SNP marker	Position Camarosa	Position Royal Royce	Protein encoded by the Candidate Gene (CG)	CG abbreviation	CG position Camarosa	F. × ananassa identity	TAIR Arabidopsis homolog	Published strawberry GWAS/QTL a
	1B	3.6	AX-184131652	4 174 690	1 302 571	Sucrose-phosphate synthase	*SPS*	4 316 703	FxaC_2g09440	AT5G20280.1	
						Sucrose-phosphate synthase	*SPS*	4 319 488	FxaC_2g09441	AT5G20280.1	
	2D	1.411	AX-184718481	13 298 291		Fructose-1,6-bisphosphatase, cytosolic	*FBP*	13 361 786	FxaC_8g25210	AT1G43670.1	
	3B	0.7	AX-184477629	1 541 393	1 842 542	∗ Starch synthase	*SS*	453 429	FxaC_10g00830	AT4G18240.1	Fan et al. (2024)
TSS (Brix)	5A	0.9–2.1	AX-184970304	12 400 711	10 544 768	Fructose-1,6-bisphosphatase, cytosolic	*FBP*	12 546 445	FxaC_17g26250	AT1G43670.1	
	6B	1.403	AX-184355355	27 647 943	10 765 128	Fructose-bisphosphate aldolase	*FBA*	27 600 407	FxaC_22g44640	AT3G52930.1	
	6B	18.96	AX-184399755	31 578 303	9 217 798	Isocitrate dehydrogenase [NAD]	*IDH*	31 758 475	FxaC_22g50900	AT5G03290.1	
	6C	0.582	AX-184221848	33 293 635	29 374 007	Aconitase	*ACO*	33 266 087	FxaC_23g56470	AT2G05710.1	
	6D	4.8	AX-184864732	12 013 420	9 512 125	Isocitrate dehydrogenase [NAD]	*IDH*	11 337 718	FxaC_24g21140	AT5G03290.1	
	7B	1.6–4.0	AX-184920058	4 515 979	19 984 301	Hexose carrier protein 6	*HEX*	4 480 262	FxaC_26g09610	AT5G61520.1	
	7C	7.718	AX-184047575	20 267 768		Alkaline/neutral invertase	*INV*	20 384 455	FxaC_27g29380	AT4G09510.1	
	7C	0.5	AX-184079508	26 901 718	13 298 291	Hexose carrier protein 6	*HEX*	27 292 700	FxaC_26g09610	AT5G61520.1	
BA ratio	6B	65.8	AX-184399755	31 578 303	9 217 798	Isocitrate dehydrogenase [NAD]	*IDH*	31 758 475	FxaC_22g50900	AT5G03290.1	
	1C	17.8	AX-184494194	11 470 545	10 966 861	Cinnamyl-alcohol dehydrogenase	*CAD*	11 709 567	FxaC_3g21930	AT4G39330.1	
						Cinnamyl-alcohol dehydrogenase	*CAD*	11 726 197	FxaC_3g21970	AT4G37970.1	
	3D	4.7–28.7	AX-184599570-AX-184177060	26 901 693–27 845 440	3 815 908–4 775 280	MYB-SHAQKYF	*MYS*	27 802 931	FxaC_12g42500	AT2G38300.1	
						Trichome birefringence-like 38	*TBL*	27 558 105	FxaC_12g42010	AT1G29050.1	
						∗ Hydroxycinnamoyl-CoA shikimate/quinate hydroxycinnamoyltransferase	*HCT*	28 432 367	FxaC_12g43430	AT5G48930.1	
Glossiness (GLOS)						∗ GDSL esterase/lipase	*GELP*	28 471 370	FxaC_12g43470	AT1G29670.1	
						∗ GDSL esterase/lipase	*GELP*	28 475 004	FxaC_12g43480	AT1G29670.1	
						∗ GDSL esterase/lipase	*GELP*	28 478 770	FxaC_12g43490	AT1G29670.1	
	4C	3.4	AX-184951955	727 143	26 073 661	Non-specific Lipid Transport Protein	*nsLTP*	756 662	FxaC_15g01440	AT2G37870.1	
						Glycerol-3-phosphate acyltransferase	*GPAT6*	901 347	FxaC_15g01830	AT2G38110.1	
	5A	4.1–11.1	AX-184408294-AX-184352835	28 658 239–28 239 789	24 966 878–25 341 723	Non-specific Lipid Transport Protein	*nsLTP*	28 693 018	FxaC_17g54360	AT5G64080.1	
						Glycerol-3-phosphate acyltransferase	*GPAT3*	28 952 583	FxaC_17g54920	AT4G01950.1	

(Continued)

Table 2. Continued

Trait	Chr	PVE	SNP marker	Position Camarosa	Position Royal Royce	Protein encoded by the Candidate Gene (CG)	CG abbreviation	CG position Camarosa	F. × ananassa identity	TAIR Arabidopsis homolog	Published strawberry GWAS/QTL a
Skin resistance (SR)	3D	8.4	AX-184177060	27 845 440	3 815 908	MYB-SHAQKYF 1	*MYS*	27 802 931	FxaC_12g42500	AT2G38300.1	
						Trichome birefringence-like 38	*TBL*	27 558 105	FxaC_12g42010	AT1G29050.1	
						∗ Hydroxycinnamoyl-CoA shikimate/quinate hydroxycinnamoyltransferase	*HCT*	28 432 367	FxaC_12g43430	AT5G48930.1	
						∗ GDSL esterase/lipase	*GELP*	28 471 370	FxaC_12g43470	AT1G29670.1	
						∗ GDSL esterase/lipase	*GELP*	28 475 004	FxaC_12g43480	AT1G29670.1	
						∗ GDSL esterase/lipase	*GELP*	28 478 770	FxaC_12g43490	AT1G29670.1	
	4A	5.4	AX-184127736	20 012 930	16 433 479	COBRA-like	*COBL*	20 088 406	FxaC_13g38300	AT4G16120.1	
						COBRA-like	*COBL*	20 089 498	FxaC_13g38301	AT4G16120.1	
						Beta-D-xylosidase	*BXL*	20 219 525	FxaC_13g38530	AT5G49360.1	
						Trichome birefringence-like 43	*TBL*	20 238 095	FxaC_13g38560	AT2G30900.1	
	5B	3.6	AX-184230747	15 853 776	12 173 853	Pectin methylesterase inhibitor	*PMEI*	15 657 184	ID=FxaC_18g23430	AT5.1G38610	
	7A	7.3	AX-184130926	25 616 815	18 667 225	Polyglacturonase	*PG*	25 398 299	FxaC_25g46610	AT2G43890.1	
						Expansin B2	*EXP*	25 744 435	FxaC_25g47360	AT1G65680.1	
						Expansin B2	*EXP*	25 766 632	FxaC_25g47430	AT1G65680.1	
						Decrease was biosynthesis 2	*DEWAX*	25 608 061	FxaC_25g47130	AT5G07580.1	
						Decrease was biosynthesis 2	*DEWAX*	25 647 466	FxaC_25g47200	AT5G07580.1	
	7A	1.6	AX-123359788	28 581 204		Wax ester synthase	*WSD*	28 523 042	FxaC_25g53661	AT3G49210.1	
Bruisedness (BRU)	1A	6.919	AX-184940044	3 531 536		Epidermal patterning factor	*EPFL*	3 396 016	FxaC_1g08100	AT3G13898.1	
	1B	6.887	AX-184203769	9 439 391	7 276 991	GDSL lipase	*GELP*	9 476 517	FxaC_2g20370	AT2G23540.1	
	5A	4.387	AX-184408176	18 814 640	16 414 924	Pectate lyase	*PL*	18 712 472	FxaC_17g36850	AT5G09280.1	
	6B	5.489	AX-184399480	5 731 875	30 532 752	Fasciclin-like arabinogalactan protein	*FLA*	5 305 159	FxaC_22g11190	AT5G06920.1	
						Fasciclin-like arabinogalactan protein	*FLA*	5 332 088	FxaC_22g11250	AT5G06920.1	
						Xyloglucan endotransglucosylase/hydrolase	*XTH*	5 351 858	FxaC_22g11330	AT4G03210.1	
	7C	2.8	AX-184713611	20 943 204	15 149 370	3-ketoacyl-CoA synthase 1-like	*KCS*	20 714 519	FxaC_27g29940	AT1G01120.1	

[a] Publications: Natarajan et al. (2020) [41], Alarfaj et al. (2021) [40], Cockerton et al. (2021) [17], Hardigan et al. (2021b) [4], Rey-Serra et al. (2021) [15], Fan et al. (2023) [29], Fan et al. (2024) [31], Muñoz et al. (2024) [39].
PVE, Phenotypic variance explained (%). Position Camarosa and Position Royal Royce: physical positions on Camarosa and Royal Royce reference genomes. Protein encoded by the candidate gene (CG): annotation in the Camarosa genome. CG Position Camarosa and *F.* × *ananassa* identity: physical position and identity in the Camarosa genome. Published GWAS/QTL: QTL detected with Affymetrix strawberry arrays on the same chromosomal regions as in this study.
∗ CG found outside ∼400 kb intervals around SNP markers.

regions were detected here (Table 2). Our AX-184039356 marker linked to FIRM on 6A is very close to those previously described for fruit firmness [4, 17, 31, 39]. Likewise, our AX-184477629 marker linked to TSS on 3B is in the same chromosomal region as the SSC1 QTL controlling soluble solid content [31]. In contrast, several previously reported QTL such as a FW QTL on 5B [29, 41], a TSS QTL on 5A [41], and a TA QTL on 5A [15] have been found on the same chromosomes but in different regions. The genetic diversity of unique European accessions included in our study allowed us to reveal new QTL and associated SNP markers, even for well-studied fruit quality traits such as FW and TSS.

In contrast to these well-studied traits, few studies have unveiled the genetic architecture of skin associated traits such as fruit glossiness [17, 42] which is, alongside color, one of the most prominent traits for fruit attractiveness to the consumer [43]. Remarkably, of the seven associations found among the six selective sweeps detected, two were found for GLOS and two for SR (Fig. 5A). Furthermore, by highlighting a ~6400 kb region on chromosome 3D linked to glossiness, skin resistance, and firmness, our results shed a new light on a genomic region under strong breeding pressure (Figs. 1F, 5A). This chromosomal region has thus probably played a crucial role in improving the attractiveness and postharvest qualities of strawberries, a feature that is receiving increasing attention in strawberry breeding programs. Information on the position of SNP markers on both Camarosa and Royal Royce genomes will facilitate new studies on fruit quality traits, thus contributing to validate these markers for MAS.

Candidate genes

Fruit weight and appearance

FW and shape are complex traits. Underlying genes of previously unknown functions have been identified by map-based cloning in species such as tomato [44], and corresponding CG have been detected in several crops [45]. Translation of these findings to strawberry may however prove difficult because of the different ontogenic origins of strawberry, which is an accessory fruit derived from the flower receptacle and not from the ovary. Indeed, our GWAS study did not detect any known gene families linked to fruit weight and shape, but highlighted for FW QTL several CG (*CDKE*, a cluster of five *SAUR*, *CUL*) involved in cell division and expansion processes and their regulation (Table S5).

Red-colored anthocyanins, which give strawberries their attractive bright red appearance, are flavonoids derived from the phenylpropanoid pathway. In cultivated strawberry, allelic variants of the master regulator *MYB10* belonging to the MBW complex have been shown to be responsible for the white skin color and red flesh color [8, 11]. In our GWAS study, we did not detect any previously known color QTL nor CG linked to the MBW complex, probably because white fruit genotypes and flesh color trait were under-represented in our analysis. However, our diversity panel has enabled us to reveal new skin color QTLs and identify strong CG involved in the successive steps leading to anthocyanin accumulation in strawberry [11]: (i) anthocyanin biosynthesis; (ii) formation of stabilized anthocyanidin-glucosides; and (iii) transport of anthocyanidin-glucosides for storage in the vacuole. Color CG, which deserve further study, include a gene (*CSE*) encoding shikimate esterase, an enzyme involved in lignin pathway that may compete with anthocyanin biosynthesis for common substrates; several genes encoding glycosyltransferases (*GT*), among which the strawberry FaGT1 enzyme, which has been shown to generate anthocyanidin 3-O-glucosides [46] and its homolog FaGT2; and a gene encoding a vacuolar flavonoid/H+-antiporter (*TT12*), which can actively transport cyanidin-3-O-glucoside to the vacuole [47].

Fruit firmness and composition

Breakdown of the cell wall (CW) is the main mechanism responsible for fruit softening during ripening. CW is mainly constituted by a cellulose–hemicellulose network immersed in a pectin matrix. Strawberry fruit softening involves the pectin-degrading enzymes polygalacturonase (PG) and pectate lyase (PL) [48]. The downregulation of *PL* [49] and of *PG* [50] influences fruit firmness and/or shelf life of strawberry. Many additional proteins are involved in CW modifications, e.g. pectin methylesterase (PME) and its inhibitors (PMEI) that control cell adhesion and elasticity through pectin esterification, enzymes of the xyloglucan endotransglycosylase/hydrolase (XTH) family involved in hemicellulose remodelling, cellulases (CEL) that degrade cellulose, and expansins (EXP) that promote CW loosening. Other enzymes such as cellulose synthase (CES) or proteins with ill-defined roles such as arabinogalactan-proteins (AGPs) likely play a role in CW structure and properties. Therefore, considerable variations in fruit firmness can be expected by modulating the activity of enzymes encoded by CG underlying the 3D QTL (*GALT, XTH, CES*) and 6A (*CEL, PG*) QTL. *XTH* and *CES* are strong candidates located at 750 to 1280 kb from the AX-184477554 marker in the well-conserved 3D region while *CEL* and *PG* underly the 6D FIRM QTL previously detected [4].

The sugar/acid balance is central for consumer perception of fruit quality [19] and the sugar/acid ratio has been widely adopted as a breeding target [5]. The major soluble sugars that accumulate during fruit ripening are glucose, fructose, and sucrose, the concentration of which depends on the cultivar [51]. The major organic acids are malate and especially citrate, which is the predominant organic acid [48]. Their concentrations are stable or decrease during fruit ripening. Fruit sweetness is usually assessed in refractometer (Brix units), which measures total soluble solids (TSS), including sugars and organic acids. Fruit acidity is assessed by TA, to which citrate contributes most in strawberry. The accumulation in strawberry of soluble sugars and organic acids depends on synthesis in the leaf (source) and long-distance transport of photoassimilates (sucrose, inositol) to the fruit (sink). Photosynthetic sugars are further metabolized in the fruit to produce soluble sugars and organic acids that are then stored in the vacuoles [52]. Our GWAS study identified several CG implicated in the metabolism of sugars, either in the leaves or in the fruit, including *SPS* (1B QTL), *FBP* (2D and 5A QTL), *SS* (3B QTL), *FBA* (6B QTL), and *INV* (7C QTL). The starch synthase (*SS*) is located >1 Mb apart from the 3B QTL marker but has been recently identified as a CG for a TSS QTL [31]. The neutral invertase (*INV*), which underlies the major 7C TSS QTL (PVE 7.7%), is a strong candidate that has been shown to be crucial for glucose and fructose accumulation during ripening in tomato [53] while a CW invertase is responsible for a major TSS QTL in this species [54]. Another strong candidate is the hexose transporter (*HEX*) (7B and 7C QTL), which could transport glucose and fructose across the tonoplast, as suggested in grape berries [55]. Furthermore, the *HEX* gene may underlie two possible TSS homoeo-QTL located on chromosomes 7B and 7C, respectively.

Two CG underlying TSS QTL encode enzymes involved in the tricarboxylic acid (TCA) cycle, notably isocitrate dehydrogenase [NAD] (IDH) (6B QTL) and aconitase (ACO) (6C QTL). TCA is the central metabolic cycle that uses substrates from the glycolysis to produce energy. It fulfills major roles in the fruit, among which is the metabolism of citric acid [56]. While ACO has been shown to

contribute to the regulation of acidity in the citrate-accumulating lemon [57], we did not detect any TA QTL corresponding to the 6C Brix QTL. Interestingly, *IDH* underlies strong shared QTL for TSS (PVE = 19.0) and BA (PVE = 65.8) on chromosome 6B. The implication of IDH a significant contributor to the TCA cycle, in the sugar/acid balance of strawberry, therefore merits further studies. Moreover, *IDH* is also located at ~675 kb from the TSS QTL on chromosome 6D, indicating that it could underlie two TSS homoeo-QTL located on chromosome 6B and 6D, respectively. As previously suggested [13], the detection of homoeo-QTL could depend on environmental conditions, which vary according to the year of study.

The CG underlying the 1A TA QTL encodes pyruvate kinase (PK), a crucial enzyme for gluconeogenesis, which has already been demonstrated to regulate citric acid metabolism during strawberry fruit ripening [56]. Two additional CG for the TA QTL located on 6A (PVE 35.3%) and 6C (PVE 6.8%) encode subunits of the V-type proton ATPase (*VMA-G* and *VMA-C*), respectively. Both are strong candidates for the control of fruit acidity, as they are part of a protein complex whose role is to generate a proton gradient across the tonoplast, which is essential to drive the storage of organic acids in the vacuole of fleshy fruits [58].

Skin properties

The outermost wall of the fruit is composed of the cuticle, the epidermis and several layers of subepidermal cells [59]. This ill-defined tissue, also called fruit skin [60], acts as a barrier against water loss and pathogens and provides protection against mechanical injuries [61]. Its properties depend on epidermal and subepidermal cell patterning (cell size and shape) and on the composition and structure of CW and cuticle. To date, the cuticle has been poorly studied in strawberry, except for its composition [62]. Recent studies, in particular in the tomato model, furthered our understanding of the synthesis of cuticle components (wax and cutin polyester, phenolics) and explored the complex interactions between cutin polyesters, CW polysaccharides, and phenolics and their possible contribution to cuticle properties [59].

Fruit glossiness is an environment-sensitive trait linked to wax and cutin accumulation on the fruit surface but also to epidermal cell patterning [63]. Among CG identified for GLOS QTL are genes involved in phenylpropanoid pathways (*CAD* in 1C QTL), epidermal patterning (*TBL* in 3D QTL), regulation of wax biosynthesis (MYS, 3D QTL), lipid and cutin biosynthesis (GPAT6, 4C QTL; GPAT3, 5A QTL), and possibly transport of cutin precursors (nsLTP, 4C and 5A) [61, 64]. In addition to the *MYS* gene, a transcription factor involved through *DEWAX* in the regulation of the ECERIFERUM1 (CER1) enzyme involved in the biosynthesis of wax alkanes [65], this region harbors, within ~700 kb of 3D QTL markers, the phenolic pathway *HCT* gene that is essential for cuticle formation [66] and, close-by, three *GELP* genes. Several members of the large *GELP* family have been demonstrated to play crucial roles in cutin polymerization (cutin synthase [67]) and in assembly–disassembly of the related polyester suberin [68]. Examination at the Tomato eFP Browser (http://bar.utoronto.ca) and TEA-SGN (https://tea.solgenomics.net) databases of the expression of the three closest tomato homologs (*Solyc03g005900, Solyc02g071610, Solyc02g071620*) of the 3D GLOS QTL-linked *GELP* genes indicate that they are strongly expressed in the young fruit, when the cutin synthesis rate is the highest [63]. Furthermore, in the tomato pericarp, their expression is restricted to the outer and inner epidermis. These findings strongly suggest that, in cultivated strawberry, a cluster of genes with likely roles in cuticle formation and structure has been selected in modern varieties for its impact on fruit cuticle-related traits, including GLOS.

Remarkably, we found that the major skin resistance (SR) QTL, which estimates the fragility of the fruit surface to peel off when a mechanical stress is applied, is shared with the GLOS QTL on 3D. The major 3D FIRM QTL (PVE 11.2%) was also found nearby (at ~1400 kb). Since the FIRM trait was estimated by measuring the force needed to punch a hole in the fruit surface (penetrometer), it can be linked to the properties of the fruit skin. Interestingly, connections between fruit firmness and the cuticle have recently been demonstrated in tomato, where changes in cuticle composition and properties are responsible for a major firmness QTL [69]. Altogether, these results suggest that in the 3D conserved region, modifications of fruit surface properties, either due to changes in epidermal cell patterning and/or in CW and cuticle properties, have been selected in modern strawberry varieties for their effect on both fruit glossiness, resistance to mechanical damages, and possibly firmness. Other candidates linked to either epidermis patterning (*TBL* on 4A), CW modifications (*COBL* and *BXL* on 4A, *PMEI* on 5C, *PG* and *EXP* on 7A), and cuticle formation (*DEWAX*, a target of MYS, and *WSD* on 7A) underlie the additional SR QTL detected.

In contrast, none of the QTL detected for fruit bruisedness (BRU), a trait assessed visually, were found to colocalize with either GLOS, SR, or FIRM QTL while all these traits are strongly correlated, indicating that the underlying mechanisms are probably different or that the corresponding QTL are below the detection threshold. CW-related GC that may affect CW properties (*PL* on 5A, *XTH* on 6B) or cell adhesion of subepidermal cells (*FLA* on 6B [70]) merit further investigation, as fruit susceptibility to bruising is essential for postharvest handling and defense against fruit decay.

Conclusion

In summary, the exploration of untapped genetic resources, including European cultivars spanning 160 years of breeding, has revealed considerable changes in recent decades in the genetic and phenotypic diversity of cultivated strawberry. American cultivars have had a major impact on recent European breeding programs and, therefore, on modern strawberry varieties in Europe. However, our findings also revealed that a considerable, and previously undescribed, genetic diversity can be harnessed for improving fruit quality through breeding. Our study also highlights the contribution of fruit surface traits (glossiness, skin resistance, bruisedness) to the development of modern varieties. The strong CGs underlying the main QTL detected for these little-studied traits warrant further investigations. This can be done, for example, through additional association studies or functional analyses. From a more applied perspective, the genetic markers highlighted will be used for the selection of improved strawberry varieties with high fruit quality.

Materials and methods

Plant materials and experimental design

A total of 223 accessions from the historical germplasm collection of Invenio was chosen to constitute the diversity panel. The trial took place in a soilless system, at Douville in the South-West of France (45° 1.2831' N; 0° 37.0198' E, France). The crop management was the one used for commercial semi-early cultivated strawberry in France. The trial was organized in a randomized complete block design of two blocks of four biological replicates each in a 288

m^2 glass greenhouse in 2020 and 2021. Planting of tray plants occurred around 15 December of the previous year.

Sample preparation and phenotyping

Fruits were harvested once per season and evaluated for 12 fruit quality traits: FW, fruit weight; UFS, uniformity of fruit shape; COL, skin color; UCOL, uniformity of skin color; ACH, position of achenes; FIRM, firmness; TA, titratable acidity; TSS, total soluble solids; BA, TSS/TA ratio; GLOS, glossiness; SR, skin resistance; and BRU, bruisedness. FW was evaluated as the mean weight of harvested fruits after discarding immature and over-ripe fruits. UFS, UCOL, ACH, as well as GLOS and BRU were visually assessed on 1–5 scales (Table 1) as a single note on a whole strawberry tray (>10 red ripe fruits). COL was evaluated on 4–5 red ripe fruits on a 1–8 scale based on the strawberry color chart from Ctifl (http://www.ctifl.fr/Pages/Kiosque/DetailsOuvrage.aspx?IdType=3&idouvrage=833). FIRM was evaluated on six fruits from each accession with an FTA-GS15 (Güss) penetrometer (5 mm diameter) at 3 mm depth (5 mm/s speed, 0.06 kg release threshold). SR was evaluated on three fruits per accession on a 1–5 scale by applying an ascending pressure with the extremity of the thumb on the fruit surface. Bruisedness, which represents the susceptibility of the fruit to mechanical damages, was evaluated by visual inspection of the fruits 4 h after harvest. Analyses were performed for two consecutive years except for FIRM and SR traits, which were evaluated a single year in 2021. TA and TSS were evaluated from a homogenized pool of a minimum of 10 fruits with a pH-metric titration with sodium hydroxide of 10-g fruit puree and an Atago Handheld (PAL-1) Digital Pocket Refractometer (Atago, Saitama, Japan), respectively.

Statistical analysis

Best Unbiased Linear Predictors (BLUPs) for the diversity panel were calculated using a linear mixed model (LMM) from the lme4 R package [71]:

$$yijkl = \mu + \underline{G}i + Bk + Yl + (G:Y)il + \epsilon ikl,$$

where Y/E represented the fixed effects of year/environments; B the fixed effect of blocks; G the random genotypic effect, with $G \sim N(0, \sigma g^2 I)$; GxY/E the random genotype × year/environment effects, with $GxY/E \sim N(0, \sigma Y/E^2 I)$; ϵ the residual term, with $e \sim N(0, \sigma e^2 I)$.

Variance components for these effects were estimated using restricted maximum likelihood (REML).

Broad sense heritability was estimated as follows:

$$H^2 = \frac{\sigma^2 G}{\sigma^2 G + \frac{\sigma^2 G:Y}{nyear} + \frac{\sigma^2 e}{nyear \times nrep.year}}$$

where genotype (G) variance at the numerator. Random variance components involving year (Y) were divided by the mean number of years (*nyear*). Other random variance components involving block effects or residuals were divided by the mean number of years times the mean number of replicates per year (*nrep.year*).

Pearson correlation between different traits were calculated using 'cor' function and visualized by 'corrplot' v. 0.92 R package. PCA on all traits was performed using the prcomp function from R core and visualized with fviz_pca function from factoextra v.1.0.7 package or ggplot2 package. The impact of the structure on each variable was assessed by simple regression of the genetic groups on their respective phenotypes.

Genotyping

DNA was extracted from young leaves with a CTAB method adapted from Sánchez-Sevilla et al. (2015) [34]. Samples were genotyped using Affymetrix® 50 K FanaSNP array [22] in the 'Gentyane' genotyping platform (Clermont-Auvergne-Rhône-Alpes, INRAE, France). SNP calling was processed through Axiom™ Analysis Suite software (v5.1.1.1; Thermo Fisher Scientific, Inc.) following the best practices of the software documentation. Accessions with missing data >3% were removed from analysis. Markers presenting >5% of missing data and minor allele frequencies of <5% were filtered out.

Structure and genetic diversity analysis

We performed a structure population analysis using STRUCTURE (v2.3.4 [72]) with 5 runs for a range of K = 2–10 with 38 120 markers. The burn-in period length was set to 10 000 and 20 000 Markov Chain Monte Carlo (MCMC). The best fitting K was identified with STRUCTURE HARVESTER [73]. Plots were performed using the ggplot2 v.3.3.6 package [74]. PCA analyses were performed with PCA function from factorMinerR v.2.7 package [75]. Additionally, we included genotypes from Hardigan et al., (2021b) [4] and Zurn et al. (2022) [28] to perform PCA using the prcomp function from R core and visualize with fviz_pca_ind function from factoextra v.1.0.7 package or ggplot2 package. We conducted a ML tree with the 233 accessions using IQ-TREE v.2.1.3 [76] with 1000 bootstrap and the TVMe+ASC + R3 model suitable for SNP arrays. LD for each chromosome and genetic group was computed using the LDcorSV v.1.3.3 package [77]. Nucleotide diversity among each genetic group was calculated using TASSEL [78]. Finally, we performed principal component analysis-based genomes scans to detect markers under selection using the pcadapt package [79], implementing the pcadapt function with K = 3. Outputs from genome scans were then compared with nucleotide diversity profiles to search for selective sweeps.

Genome-wide association study

The association mapping was performed using GAPIT v.3 [80] using the Camarosa genome physical positions [1] with the Bayesian-information and linkage-disequilibrium iteratively nested keyway (BLINK) model [81]. In order to control for confounding effects, the structure was implemented for each trait in two different ways by 1) adding the previously calculated structure parameters as covariates or 2) fitting directly principal components from the principal component analysis using the PCA.total argument. Best models were selected based on genomic inflation factors, λ. The kinship was determined from the SNP data using the VanRaden mean algorithm. The analysis was performed on yearly and across 2 years Best Linear Unbiased Predictors (BLUPs), using a 5% Bonferroni threshold. Manhattan and Quantile–Quantile plots were plotted using the CMplot R package. Allelic effects for each significant marker were plotted on adjusted means using the ggplot2 R package.

Candidate gene mining

CG underlying fruit-quality QTL were identified in intervals of ~400 kb around the QTL marker. This value, which corresponds to the short-range LD found in California cultivars of *F.* × *ananassa* [4], is stringent compared to the average LD of 932 kb calculated in our diversity panel. In chromosomal regions harboring strong QTL of interest and displaying low genetic diversity and high LD, larger intervals (up to 1382 kb) were considered. The annotations of genes located within the QTL interval were retrieved from

F. × *ananassa* cv. Camarosa reference genome assembly v1.0[1] and cv. Royal Royce haplotype-resolved genome v1.0 assembly [23]. Based on the authors' expertise in fruit biology, QTL intervals were first inspected manually for genes belonging to categories possibly related to fruit quality traits, e.g. enzymes, transporters, and regulators of anthocyanin biosynthesis for fruit color [11, 14, 18], enzymes and regulators of wax and cutin biosynthesis pathways for glossiness and skin resistance [59, 61, 63, 64, 67], and enzymes of primary metabolism, organic acid transporters, and proton pumps for titratable acidity [13, 51, 82–84]. Their function in plant and fruit was then investigated by exploiting the Arabidopsis database (https://www.arabidopsis.org/) with corresponding TAIR accession numbers; the relevant literature, especially that relating to strawberry and other fleshy fruit species of the *Rosaceae* family; and gene expression patterns in strawberry fruit using *F. vesca* eFP browser [85]. For skin-associated traits, patterns of gene expression in plant organs and fruit cell types were further investigated in tomato, the fleshy fruit and cuticle model, using SGN-TEA (https://tea.solgenomics.net/) and Tomato eFP browser (http://bar.utoronto.ca/efp2/Tomato/Tomato_eFPBrowser2.html).

Acknowledgements

We thank Sarah Touzani and Eva Bouillon for their help in phenotyping. The project was funded by the Nouvelle-Aquitaine Region and the European Regional Development Fund (ERDF) (REGINA project no. 67822110; AgirClim project No. 2018-1R20202); and European Union Horizon 2020 research and innovation program (BreedingValue project No. 101000747; PRIMA-Partnership 2019–22 Med-Berry project). Al.P. was supported by the CIFRE (Convention Industrielle de Formation par la Recherche) contract between Invenio (SME, Bordeaux, France) and the INRAE BAP department.

Author's contributions

B.D. and Al.P. conceived and designed the experiments. Al.P. conducted hands-on experiments and data collection. Au.P., Jo.P., and Ju.P. contributed to data collection. Al.P., P.R.S., B.D., and C.R. analyzed the data. Al.P., B.D., and C.R. wrote the original draft. All authors read and approved the final manuscript.

Data availability

All relevant data generated or analyzed are included in the manuscript and the supporting materials.

Conflict of interest statement

The authors declare that there are no conflicts of interest.

Supplementary Data

Supplementary data is available at *Horticulture Research* online.

References

1. Edger PP, Poorten TJ, VanBuren R. *et al.* Origin and evolution of the octoploid strawberry genome. *Nat Genet*. 2019;**51**:541–7
2. Whitaker VM, Knapp SJ, Hardigan MA. *et al.* A roadmap for research in octoploid strawberry. *Hortic Res*. 2020;**7**:33
3. Pincot DDA, Ledda M, Feldmann MJ. *et al.* Social network analysis of the genealogy of strawberry: retracing the wild roots of heirloom and modern cultivars. *G3 (Bethesda)*. 2021;**11**:jkab015. https://doi.org/10.1093/g3journal/jkab015
4. Hardigan MA, Lorant A, Pincot DDA. *et al.* Unraveling the complex hybrid ancestry and domestication history of cultivated strawberry. *Mol Biol Evol*. 2021b;**38**:2285–305
5. Feldmann MJ, Pincot DDA, Cole GS. *et al.* Genetic gains underpinning a little-known strawberry green revolution. *Nat Commun*. 2024;**15**:2468
6. Senger E, Osorio S, Olbricht K. *et al.* Towards smart and sustainable development of modern berry cultivars in Europe. *Plant J*. 2022;**111**:1238–51
7. Liu Z, Liang T, Kang C. Molecular bases of strawberry fruit quality traits: advances, challenges, and opportunities. *Plant Physiol*. 2023;**193**:900–14
8. Castillejo C, Waurich V, Wagner H. *et al.* Allelic variation of MYB10 is the major force controlling natural variation of skin and flesh color in strawberry (Fragaria spp.) fruit. *Plant Cell*. 2020;**32**:3723–49
9. Fan, Tieman DM, Knapp SJ. *et al.* A multi-omics framework reveals strawberry flavor genes and their regulatory elements. *New Phytol*. 2022;**236**:1089–107
10. Lara I, Belge B, Goulao LF. A focus on the biosynthesis and composition of cuticle in fruits. *J Agric Food Chem*. 2015;**63**:4005–19
11. Denoyes B, Prohaska A, Petit J. *et al.* Deciphering the genetic architecture of fruit color in strawberry. *J Exp Bot*. 2023;**74**:6306–20
12. Zorrilla-Fontanesi Y, Cabeza A, Domínguez P. *et al.* Quantitative trait loci and underlying candidate genes controlling agronomical and fruit quality traits in octoploid strawberry (Fragaria × ananassa). *Theor Appl Genet*. 2011;**123**:755–78
13. Lerceteau-Köhler E, Moing A, Guérin G. *et al.* Genetic dissection of fruit quality traits in the octoploid cultivated strawberry highlights the role of homoeo-QTL in their control. *Theor Appl Genet*. 2012;**124**:1059–77
14. Labadie M, Vallin G, Petit A. *et al.* Metabolite quantitative trait loci for flavonoids provide new insights into the genetic architecture of strawberry (Fragaria × ananassa) fruit quality. *J Agric Food Chem*. 2020;**68**:6927–39
15. Rey-Serra P, Mnejja M, Monfort A. Shape, firmness and fruit quality QTLs shared in two non-related strawberry populations. *Plant Sci*. 2021;**311**:111010
16. Muñoz P, Castillejo C, Gómez JA. *et al.* QTL analysis for ascorbic acid content in strawberry fruit reveals a complex genetic architecture and association with GDP-L-galactose phosphorylase. *Hortic Res*. 2023;**10**:uhad006
17. Cockerton HM, Karlström A, Johnson AW. *et al.* Genomic informed breeding strategies for strawberry yield and fruit quality traits. *Front Plant Sci*. 2021;**12**:724847
18. Labadie M, Vallin G, Potier A. *et al.* High resolution quantitative trait locus mapping and whole genome sequencing enable the design of an anthocyanidin reductase-specific homoeo-allelic marker for fruit colour improvement in octoploid strawberry (Fragaria × ananassa). *Front Plant Sci*. 2022;**13**:869655
19. Gaston A, Osorio S, Denoyes B. *et al.* Applying the Solanaceae strategies to strawberry crop improvement. *Trends Plant Sci*. 2020;**25**:130–40
20. Jin X, Du H, Zhu C. *et al.* Haplotype-resolved genomes of wild octoploid progenitors illuminate genomic diversifications from wild relatives to cultivated strawberry. *Nat Plants*. 2023;**9**:1252–66
21. Session AM, Rokhsar DS. Transposon signatures of allopolyploid genome evolution. *Nat Commun*. 2023;**14**:3180
22. Hardigan MA, Feldmann MJ, Lorant A. *et al.* Genome synteny has been conserved among the octoploid progenitors of cultivated

strawberry over millions of years of evolution. *Front Plant Sci*. 2020;**10**:1789
23. Hardigan MA, Feldmann MJ, Pincot DDA. *et al.* Blueprint for phasing and assembling the genomes of heterozygous polyploids: application to the octoploid genome of strawberry. *bioRxiv* 2021.11.03.467115; [Preprint]
24. Lee HE, Manivannan A, Lee SY. *et al.* Chromosome level assembly of homozygous inbred line 'Wongyo 3115' facilitates the construction of a high-density linkage map and identification of QTLs associated with fruit firmness in octoploid strawberry (Fragaria × ananassa). *Front Plant Sci*. 2021;**12**:696229
25. Han H, Barbey CR, Fan Z. *et al.* Telomere-to-telomere and haplotype-phased genome assemblies of the heterozygous octoploid 'Florida brilliance' strawberry (Fragaria × ananassa). *bioRxiv 2022.10.05.509768*
26. Mao JX, Wang Y, Wang BT. *et al.* High-quality haplotype-resolved genome assembly of cultivated octoploid strawberry. *Horticulture Research*. 2023;**10**:uhad002
27. Hummer K, Bassil NV, Zurn J. *et al.* Phenotypic characterization of a strawberry (Fragaria ×ananassa Duchesne ex Rosier) diversity collection. *Plants, People, Planet*. 2022;**5**:209–24
28. Zurn JD, Hummer KE, Bassil NV. Exploring the diversity and genetic structure of the U.S. National Cultivated Strawberry Collection. *Hortic Res*. 2022;**9**:uhac125
29. Fan Z, Whitaker VM. Genomic signatures of strawberry domestication and diversification. *Plant Cell*. 2023;**36**:1622–36
30. Oh Y, Barbey CR, Chandra S. *et al.* Genomic characterization of the fruity aroma gene, FaFAD1, reveals a gene dosage effect on γ-decalactone production in strawberry (Fragaria × ananassa). *Front Plant Sci*. 2021;**12**:639345
31. Fan Z, Verma S, Lee H. *et al.* Strawberry soluble solids QTL with inverse effects on yield. *Horticulture Research*. 2024;**11**:uhad271
32. Horvath A, Sánchez-Sevilla JF, Punelli F. *et al.* Structured diversity in octoploid strawberry cultivars: importance of the old European germplasm. *Ann Appl Biol*. 2011;**159**:358–71
33. Edger PP, VanBuren R, Colle M. *et al.* Single-molecule sequencing and optical mapping yields an improved genome of woodland strawberry (Fragaria vesca) with chromosome-scale contiguity. *Gigascience*. 2018;**7**:1–7
34. Sánchez-Sevilla JF, Horvath A, Botella MA. *et al.* Diversity arrays technology (DArT) marker platforms for diversity analysis and linkage mapping in a complex crop, the octoploid cultivated strawberry (Fragaria × ananassa). *PLoS One*. 2015;**10**:e0144960
35. Rosati P. Recent trends in strawberry production and research: an overview. *Acta Hortic*. 1993;**348**:23–44
36. Mezzetti B, Giampieri F, Zhang YT. *et al.* Status of strawberry breeding programs and cultivation systems in Europe and the rest of the world. *J Berry Res*. 2018;**8**:205–21
37. Davik J, Aaby K, Buti M. *et al.* Major-effect candidate genes identified in cultivated strawberry (Fragaria × ananassa Duch.) for ellagic acid deoxyhexoside and pelargonidin-3-O-malonylglucoside biosynthesis, key polyphenolic compounds. *Hortic Res*. 2020;**7**:125 Published 2020 Aug 1
38. Nagamatsu S, Tsubone M, Wada T. *et al.* Strawberry fruit shape: quantification by image analysis and QTL detection by genome-wide association analysis. *Breed Sci*. 2021;**71**:167–75
39. Muñoz P, Roldán-Guerra FJ, Verma S. *et al.* Genome-wide association studies in a diverse strawberry collection unveil loci controlling agronomic and fruit quality traits. *bioRxiv* 2024.03.11.584394; [Preprint]
40. Alarfaj R, El-Soda M, Antanaviciute L. *et al.* Mapping QTL underlying fruit quality traits in an F1 strawberry population. *J Hortic Sci Biotechnol*. 2021;**96**:634–45
41. Natarajan S, Hossain MR, Kim HT. *et al.* ddRAD-seq derived genome-wide SNPs, high density linkage map and QTLs for fruit quality traits in strawberry (Fragaria x ananassa). *3 Biotech*. 2020;**10**:353
42. Sieczko L, Masny A, Pruski K. *et al.* Multivariate assessment of cultivars' biodiversity among the Polish strawberry core collection. *Hort Sci (Prague)*. 2015;**42**:83–93
43. Lewers KS, Michael JN, Eunhee P. *et al.* Consumer preference and physiochemical analyses of fresh strawberries from ten cultivars. *International Journal of Fruit Science*. 2020;**20**:733–56
44. van der Knaap E, Chakrabarti M, Chu YH. *et al.* What lies beyond the eye: the molecular mechanisms regulating tomato fruit weight and shape. *Front Plant Sci*. 2014;**5**:227
45. Wu S, Zhang B, Keyhaninejad N. *et al.* A common genetic mechanism underlies morphological diversity in fruits and other plant organs. *Nat Commun*. 2018;**9**:4734 Published 2018 Nov 9
46. Griesser M, Hoffmann T, Bellido ML. *et al.* Redirection of flavonoid biosynthesis through the down-regulation of an anthocyanidin glucosyltransferase in ripening strawberry fruit. *Plant Physiol*. 2008;**146**:1528–39
47. Marinova K, Pourcel L, Weder B. *et al.* The Arabidopsis MATE transporter TT12 acts as a vacuolar flavonoid/H+ −antiporter active in proanthocyanidin-accumulating cells of the seed coat. *Plant Cell*. 2007;**19**:2023–38
48. Moya-León MA, Mattus-Araya E, Herrera R. Molecular events occurring during softening of strawberry fruit. *Front Plant Sci*. 2019;**10**:615
49. Jiménez-Bermúdez S, Redondo-Nevado J, Muñoz-Blanco J. *et al.* Manipulation of strawberry fruit softening by antisense expression of a pectate lyase gene. *Plant Physiol*. 2002;**128**:751–9
50. García-Gago JA, Posé S, Muñoz-Blanco J. *et al.* The polygalacturonase FaPG1 gene plays a key role in strawberry fruit softening. *Plant Signal Behav*. 2009;**4**:766–8
51. Moing A, Renaud C, Gaudillère M. *et al.* Biochemical changes during fruit development of four strawberry cultivars. *Journal of the American Society for Horticultural Science jashs*. 2001;**126**:394–403
52. Ruan YL. Sucrose metabolism: gateway to diverse carbon use and sugar signaling. *Annu Rev Plant Biol*. 2014;**65**:33–67
53. Miron D, Petreikov M, Carmi N. *et al.* Sucrose uptake, invertase localization and gene expression in developing fruit of Lycopersicon esculentum and the sucrose-accumulating Lycopersicon hirsutum. *Physiol Plant*. 2002;**115**:35–47
54. Fridman E, Carrari F, Liu YS. *et al.* Zooming in on a quantitative trait for tomato yield using interspecific introgressions. *Science*. 2004;**305**:1786–9
55. Afoufa-Bastien D, Medici A, Jeauffre J. *et al.* The Vitis vinifera sugar transporter gene family: phylogenetic overview and macroarray expression profiling. *BMC Plant Biol*. 2010;**10**:245 Published 2010 Nov 12
56. Yang M, Hou G, Peng Y. *et al.* FaGAPC2/FaPKc2.2 and FaPEPCK reveal differential citric acid metabolism regulation in late development of strawberry fruit. *Front Plant Sci*. 2023;**14**:1138865
57. Shlizerman L, Marsh K, Blumwald E. *et al.* Iron-shortage-induced increase in citric acid content and reduction of cytosolic aconitase activity in citrus fruit vesicles and calli. *Physiol Plant*. 2007;**131**:72–9
58. Huang XY, Wang CK, Zhao YW. *et al.* Mechanisms and regulation of organic acid accumulation in plant vacuoles. *Hortic Res*. 2021;**8**:227
59. Reynoud N, Petit J, Bres C. *et al.* The complex architecture of plant cuticles and its relation to multiple biological functions. *Front Plant Sci*. 2021;**12**:782773

60. Bargel H, Neinhuis C. Tomato (Lycopersicon esculentum mill.) fruit growth and ripening as related to the biomechanical properties of fruit skin and isolated cuticle. *J Exp Bot*. 2005;**56**:1049–60
61. Petit J, Bres C, Mauxion JP. *et al.* Breeding for cuticle-associated traits in crop species: traits, targets, and strategies. *J Exp Bot*. 2017;**68**:5369–87
62. Järvinen R, Kaimainen M, Kallio H. Cutin composition of selected northern berries and seeds. *Food Chem*. 2010;**122**:137–44
63. Petit J, Bres C, Just D. *et al.* Analyses of tomato fruit brightness mutants uncover both cutin-deficient and cutin-abundant mutants and a new hypomorphic allele of GDSL lipase. *Plant Physiol*. 2014;**164**:888–906
64. Petit J, Bres C, Mauxion JP. *et al.* The Glycerol-3-phosphate acyltransferase GPAT6 from tomato plays a central role in fruit cutin biosynthesis. *Plant Physiol*. 2016;**171**:894–913
65. Liu Q, Huang H, Chen Y. *et al.* Two Arabidopsis MYB-SHAQKYF transcription repressors regulate leaf wax biosynthesis via transcriptional suppression on DEWAX. *New Phytol*. 2022;**236**:2115–30
66. Kriegshauser L, Knosp S, Grienenberger E. *et al.* Function of the HYDROXYCINNAMOYL-CoA:SHIKIMATE HYDROXYCINNAMOYL TRANSFERASE is evolutionarily conserved in embryophytes. *Plant Cell*. 2021;**33**:1472–91
67. Girard AL, Mounet F, Lemaire-Chamley M. *et al.* Tomato GDSL1 is required for cutin deposition in the fruit cuticle. *Plant Cell*. 2012;**24**:3119–34
68. Ursache R, De Jesus Vieira Teixeira, Dénervaud Tendon V. *et al.* GDSL-domain proteins have key roles in suberin polymerization and degradation. *Nat Plants*. 2021;**7**:353–64
69. Li R, Sun S, Wang H. *et al.* FIS1 encodes a GA2-oxidase that regulates fruit firmness in tomato. *Nat Commun*. 2020;**11**:5844
70. Ma Y, Shafee T, Mudiyanselage AM. *et al.* Distinct functions of FASCILIN-LIKE ARABINOGALACTAN PROTEINS relate to domain structure [published correction appears in Plant Physiol. 2023 Aug 3;192(4):3203]. *Plant Physiol*. 2023;**192**:119–32
71. Bates D, Mächler M, Bolker B. *et al.* Fitting linear mixed-effects models using lme4. *J Stat Softw*. 2015;**67**:1–48
72. Pritchard JK, Stephens M, Donnelly P. Inference of population structure using multilocus genotype data. *Genetics*. 2000;**155**:945–59
73. Earl DA, vonHoldt B, M. STRUCTURE HARVESTER: a website and program for visualizing STRUCTURE output and implementing the Evanno method. *Conserv Genet Resour*. 2011;**4**:359–61
74. Wickham H *ggplot2: Elegant Graphics for Data Analysis*. Springer-Verlag New York. 2016;ISBN 978-3-319-24277-4. https://ggplot2.tidyverse.org.
75. Lê S, Josse J, Husson F. FactoMineR: a package for multivariate analysis. *J Stat Softw*. 2008;**25**:1–18
76. Minh BQ, Schmidt HA, Chernomor O. *et al.* IQ-TREE 2: new models and efficient methods for phylogenetic inference in the genomic era [published correction appears in Mol Biol Evol. 2020 Aug 1;37(8):2461]. *Mol Biol Evol*. 2020;**37**:1530–4
77. Mangin B, Siberchicot A, Nicolas S. *et al.* Novel measures of linkage disequilibrium that correct the bias due to population structure and relatedness. *Heredity (Edinb)*. 2012;**108**:285–91
78. Bradbury PJ, Zhang Z, Kroon DE. *et al.* TASSEL: software for association mapping of complex traits in diverse samples. *Bioinformatics*. 2007;**23**:2633–5
79. Luu K, Bazin E, Blum MG. Pcadapt: an R package to perform genome scans for selection based on principal component analysis. *Mol Ecol Resour*. 2017;**17**:67–77
80. Wang J, Zhang Z. GAPIT version 3: boosting power and accuracy for genomic association and prediction. *Genomics Proteomics Bioinformatics*. 2021;**19**:629–40
81. Huang M, Liu X, Zhou Y. *et al.* BLINK: a package for the next level of genome-wide association studies with both individuals and markers in the millions. *Gigascience*. 2019;**8**:giy154
82. Causse M, Duffe P, Gomez MC. *et al.* A genetic map of candidate genes and QTLs involved in tomato fruit size and composition. *J Exp Bot*. 2004;**55**:1671–85
83. Etienne C, Rothan C, Moing A. *et al.* Candidate genes and QTLs for sugar and organic acid content in peach [Prunus persica (L.) Batsch]. *Theor Appl Genet*. 2002;**105**:145–59
84. Etienne C, Moing A, Dirlewanger E. *et al.* Isolation and characterization of six peach cDNAs encoding key proteins in organic acid metabolism and solute accumulation: involvement in regulating peach fruit acidity. *Physiol Plant*. 2002;**114**:259–70
85. Hawkins C, Caruana J, Li J. *et al.* An eFP browser for visualizing strawberry fruit and flower transcriptomes. *Hortic Res*. 2017;**4**:17029